Full length article

Abnormal change in dynamic mechanical behavior of metallic glass by laser shock peening

Yansen Li [a,b,c], Yanpeng Wei [c,d], Xu Yi [e], Kun Zhang [b,c,*], Bingchen Wei [b,c,f,*]

[a] Department of Engineering Mechanics, Shijiazhuang Tiedao University, Shijiazhuang 050043, China
[b] Key Laboratory of Microgravity (National Microgravity Laboratory), Institute of Mechanics, Chinese Academy of Sciences, Beijing 100190, China
[c] School of Engineering Science, University of Chinese Academy of Sciences, Beijing 100049, China
[d] Key Laboratory for Mechanics in Fluid Solid Coupling Systems, Institute of Mechanics, Chinese Academy of Sciences, Beijing 100190, China
[e] China North Vehicle Research Institute, Beijing 100072, China
[f] Center of Materials Science and Optoelectronics Engineering, University of Chinese Academy of Sciences, Beijing 100049, China

ARTICLE INFO

ABSTRACT

Laser shock peening (LSP) has been shown to be an effective technique to improve the plasticity of metallic glasses (MGs) by inducing residual stress and structural rejuvenation. However, the microstructural evolution and viscoelastic properties of MGs after LSP remain largely unknown. In this paper, the dynamic mechanical properties of Zr-based MG before and after LSP treatment were investigated. An abnormal increase of storage modulus near the glass transition temperature (T_g) was observed after LSP. An increased deviation between the dynamic mechanical result and the quasi-point defect (QPD) theory prediction was also observed after the LSP treatment. A competing mechanism between the liquid-like region change and the pre-existing fringe-like precipitations is proposed to explain the unusual dynamic behaviors of MGs after LSP treatment. The results provide insightful information about the microstructural changes and viscoelastic properties of the MGs after LSP.

1. Introduction

Laser shock peening (LSP) is an attractive surface strengthening technique and has been shown to be beneficial for improving the mechanical properties of metallic components, such as fatigue life and plasticity [1–4]. This technique relies on a powerful compression shock wave generated by a high-energy density, very short duration laser pulse [5]. The amplitude of the shock wave is high enough to cause irrecoverable deformation until the amplitude falls below the dynamic yield strength of the material.

Due to ultra high shock pressure and extremely short loading time, LSP obviously modify the grain structure and size of polycrystalline metal materials, so as to change the mechanical properties of the material. Many researchers have paied their attention on it. For example, Zhang et al. researched the effects of multiple laser peening on the fatigue performance of Ti-6A-l4V alloy [6]. The highly tangled and densedislocation arrangements were found near the surface of LSP treatment specimen. LSP treatments with three overlapped laser spots provided three times increase in the fatigue life as compared with as cast sample. Based on a dislocation density-based con-stitutive model, Wang

et al. studied the process of grain refinement induced by LSP in metal components by a finite element method, which shown that the surface dislocation cell sizes of copper decreased exponentially with the peak pressure of shock wave increased [7]. They also pointed out that the laser spot overlap ratio of 75% made more uniform distribution of the refined dislocation cell sizes. Besides, Prabhakaran et al. studied the topographical changes induced by laser shock peening without coating in austenitic stainless steel [8]. They found many significant changes, such as increased microhardness and decreased wettability on the surface. Multidirectional mechanical twinning, dislocations lines and stacking faults were also shown in the results of TEM. Furthermore, Kalainathan et al. systematically analyzed the development of low energy LSP in recent years and believed that it was worth enough to study in the fields of metal matrix composites and single crystals [9].

However, the studies mentioned above mainly focus on the effects of LSP on crystal alloys. For metallic glasses (MGs), the absence of grain makes new response mechanisms to LSP and relevant studies are poorly reported. Although some researchers considered LSP as an effective method for reducing the brittleness of metallic glasses (MGs) due to the extra-deep residual stress region and obvious structural rejuvenation

[10–12]. For instance, Cao et al. achieved a 0.6% compression plastic increase of Zr-based MG by applying three consecutive tracks of LSP to the sample surface [13]. Ji et al. have also reported that LSP can facilitate the formation of shear bands and promote the plastic deformation of MGs [14]. Our understanding of the micro-scale response of MGs to dynamic loading remains still limited. Wang *et al.* reported that a dual-step strain variation occurred in LSP-treated MGs during quasi-static compression tests, which was related to the homogenization and annihilation of interconnected "weak spots" [15]. Zhu *et al.* measured the change in the free volume of MG after LSP in terms of structural relaxation exothermic enthalpy [16]. They attributed the decrease in hardness and increase in plasticity to the creation of excess free volume during LSP. By means of the depth-sensing method in grid nano-indentation, an abnormal change in free volume is also found in the shock-affected region of MGs in our previous work, which can be attributed to the fluctuations of the structural heterogeneity induced by the release stress wave [17]. However, this so called "weak spots" have thermodynamically and kinetically metastable nature. It has also been noted that a structural relaxation occurs when MGs are annealed below the glass transition temperature (T_g) [18], while LSP treatment can promote an obvious "rejuvenation'' phenomenon [12]. This provides an interesting opportunity to investigate the relationship between the microstructural changes and dynamic mechanical responses in MGs after LSP treatment.

In this study, the dynamic mechanical response of Zr-based MG before and after LSP was investigated by dynamic mechanical analysis (DMA). An abnormal increase in storage modulus was observed near the T_g after LSP. The origin of this unique phenomenon is discussed in detail. The LSP-induced structural changes in MG were also studied. Additionally, the effects of structural changes on the dynamic mechanical response were evaluated.

2. Experimental procedure

A master alloy of $Zr_{41.2}Ti_{13.8}Cu_{12.5}Ni_{10}Be_{22.5}$ (at.%) was prepared by arc melting the pure elemental constituents (99.99%) together in a pure argon atmosphere. The ingots were re-melted several times to ensure chemical homogeneity. Then, they were suck-casted into a water-cooled copper mold to prepare the MGs. A Q-switched Nd: YAG pulse laser with 1,064 nm wavelength was used to perform the LSP (pulse duration: 30 ns, maximum pulse energy: 2.5 J). The ablative coating layer was aluminum foil (~40 μm). Purified water was chosen as the confining medium to limit the laser irradiation.

According to our previous work [12,19–21], the higher or lower laser energy may destroy sample or weaken the effect of LSP on structure evolution. The laser power density of 4 GW/cm^2 presentes a better result, which can not only introduce a deeper plastic affect zone, but also keep sample unbroken. As a result, a large amount of free volume is induced due to microstructure change. In order to obtain the optimal effect, the same laser power density was selected in this paper. The impact spot was an approximate circle with a diameter of 2.5 mm. Moreover, a repetition rate of 50% between adjacent spots was adopted. The microstructure of the samples was examined by X-ray diffraction (XRD) analysis on a Philips PW 1050 X-ray diffractometer (Philips Electronics N.V., Amsterdam, The Netherlands) with Cu Kα radiation and transmission electron microscopy (TEM) on a FEI Tecnai G2 transmission electron microscope (FEI Co., Hillsboro, OR, USA) operating at 200 kV.

The dynamic mechanical measurements were carried out on a TA DMA Q800 dynamic mechanical analyzer (TA Instruments, New Castle, DE, USA) with a single-cantilever bending mode in a nitrogen-flushed atmosphere. The specimen was carefully pre-polished to reduce roughness and remove surface defects. To determine the temperature spectrum, DMA experiments were performed at fixed frequencies of 1, 2, 8, and 16 Hz during continuous heating from room temperature (RT) to 748 K with a constant heating rate of 3 K/min. The isothermal frequency spectrum was obtained at a given temperature with frequencies ranging from 0.1 to 16 Hz. Bar samples with a size of 35 mm × 2mm × 1mm were machined from the MG plate for the mechanical spectroscopy study.

3. Results and discussion

The temperature dependence of the storage modulus of MGs before and after LSP treatment at different loading frequencies are shown in Fig. 1. The results in Fig. 1(a) reveal that the storage modulus of the as-cast sample shows a slight change at the temperature lower than 550 K, the MG exhibits elastic behavior and the viscoelastic component is negligible. The slight decrease with increasing temperature can be attributed to the residual stress relief [22]. With further increase of the temperature, the storage modulus starts to decrease rapidly and exhibits a clear sigmoidal change near the T_g. The drastic drop in the storage modulus is associated with the mechanical relaxation related to atomic motion (reorganization of the metastable amorphous structure) as the transition from a glassy solid state to a viscous liquid occurs. The maximum change of the storage modulus usually occurs at the T_g point where two tangent lines intercept. Eventually, the storage modulus recovers and increases drastically with increasing temperature due to the crystallization. It should be noted that an abnormal increase of the storage modulus near the T_g was observed at the frequency of 16 Hz. This unique phenomenon can also be quantified as the parameter$\Delta E'/E_0'$. As shown in Fig. 1 (c), $\Delta E'/E_0'$ has a slight change at the frequencies of 1, 2, and 8 Hz, and then increases to 0.08 at 16 Hz. In addition, the temperature of T_g has a little right shift at 16 Hz, compared with other frequencies. These results on the changes of the storage modulus with frequency near the T_g are consistent with those of previous studies [23,24]. The reason for this is that the glass transition acts as an atomic relaxation that involves cooperative segmental motion whose rate depends on temperature. With the increase of the test frequency, more movement of the atoms will be required to match the applied frequency, thus the temperature of the atomic relaxations shifts to a higher temperature. Consequently, the T_g point will increase with increasing frequency. However, this is not the actual case in MG after LSP. It should be noted that a delayed fall in E' after LSP at 1 Hz can be observed in Fig. 1 (b). With the increasing frequencies, the storage modulus in turn exhibits a slight increase near the T_g compared with the as-cast samples. As shown in Fig. 1 (d), the amplitude of $\Delta E'/E_0'$ has a positive correlation with the frequency. Previous studies showed that the abnormal increase in the storage modulus near the T_g may be induced by the precipitated phase in the amorphous matrix [25–28]. Therefore, in this study, the microstructure of the samples was examined by XRD analysis (as shown in Fig. S1). For the MG before and after LSP treatment, only a broad diffraction peak, without distinct sharp crystalline peaks, can be observed, indicating their no grains exist. In addition, the second phase was also not detected in the samples that heated up to 633 K during the dynamic mechanical test.

The TEM bright field (BF) images of as-cast and LSP-treated samples, as well as the as-cast sample continuously heated up to 633 K at a frequency of 16 Hz in DMA test (also called the post-DMA sample) are shown in Fig. 2. No distinct contrast is observed in the as-cast sample, and the corresponding selected area electron diffraction (SAED) pattern shows a broad diffraction halo, implying that the structure of the as-cast sample was completely amorphous. The HRTEM micrograph displayed in Fig. 2 (b) also confirms the amorphous structure without any nanocrystallization. The TEM image of the LSP-treated sample displayed in Fig. 2 (c) shows no significant change in the BF image and a SAED pattern is observed except that the diameter of the diffraction halo is increased from 0.8398 1/Å to 0.8489 1/Å. In fact, the size of the diffraction ring corresponds to the average atomic distance in amorphous systems [29]. The change in the diffraction halo indicated that a shrinking of the mean nearest neighbor atomic spacing had occurred due to the LSP-induced residual stress. In addition, the microstructure of the LSP-treated sample was further analyzed by HRTEM analysis. Lattice
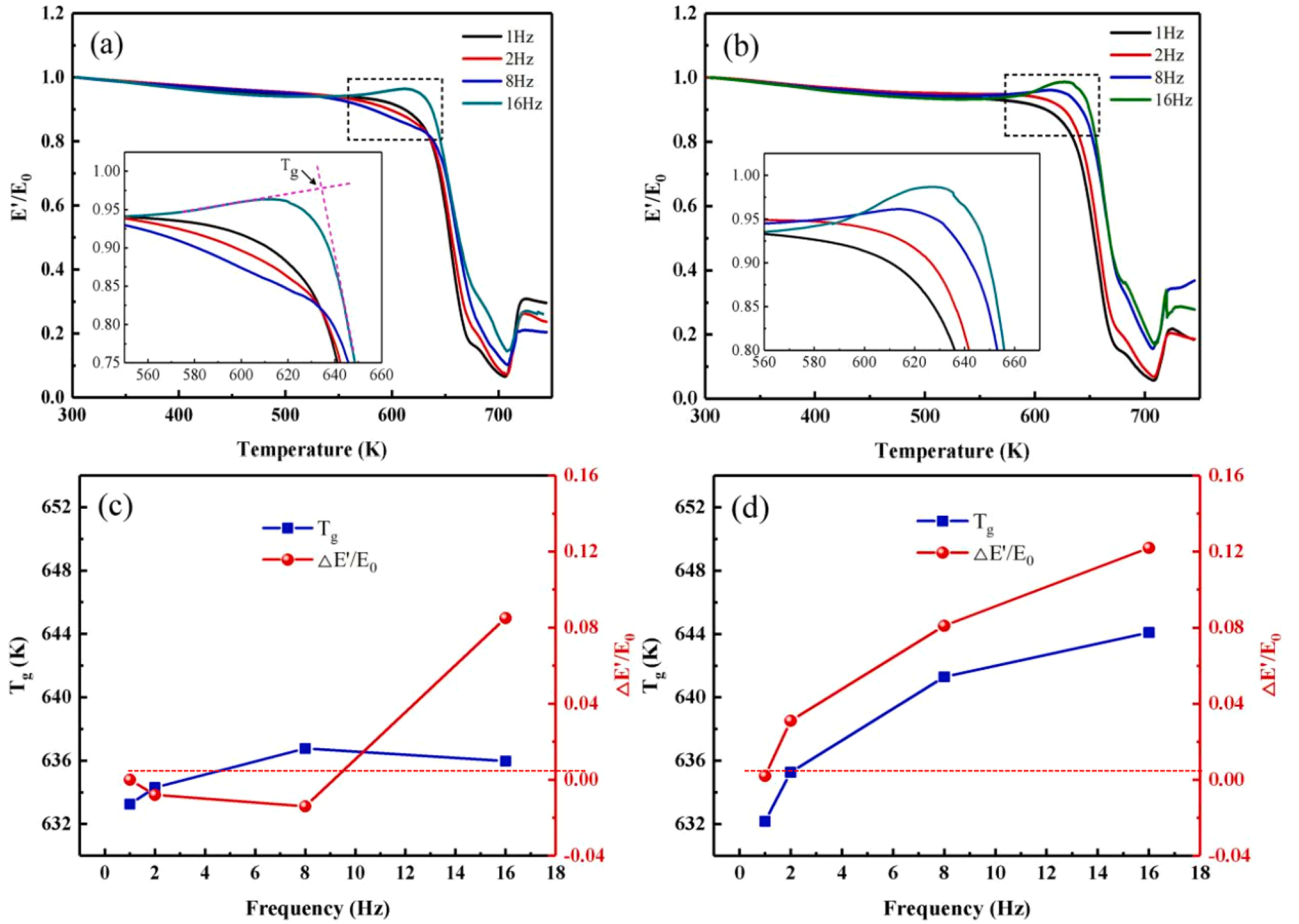
Fig. 1. Temperature dependence of storage modulus at different frequencies: (a) as-cast samples, (b) LSP-treated samples. The inset is an enlarged version of the marked area. E_0 denotes the initial storage modulus at RT and T_g is the glass transition temperature. The variation of the T_g and the different values of the storage modulus with respect to the as-cast sample under 1 Hz at the T_g: (c) as-cast samples, (d) LSP-treated samples.

fringe-like precipitations of less than 3 nm are observed, which are clear evidence of the formation of a crystal-like ordered structure in a short-range scale. The TEM image of the post-DMA sample is shown in Fig. 2 (e) for comparison. It reveals that the diameter of the diffraction halo in the post-DMA sample shows a similar trend as the LSP-treated sample, which increases from 0.8398 1/Å to 0.8544 1/Å. Although both methods lead to the densification of the atomic structure, the process occurs through entirely different mechanisms. The compression residual stress induced by LSP results in atomic compaction in the MG samples, but the atomic densification during the DMA test is the result of relaxation, accompanied by the transition of the atom from its non-equilibrium state to its equilibrium state. More importantly, the length of the lattice fringe-like precipitations increased to a large scale (exceed to 5 nm) in the post-DMA samples, which corresponds to the obvious phase transformation that occurs during the dynamic relaxation at a high frequency. Martin et al. reported that the amorphous structure still retained a maze pattern in the HRTEM image if the samples were annealed near T_g [30]. The result does not reveal the reason for the thermal-induced structural transformation during dynamic mechanical loading. Therefore, the appearance of the lattice fringe-like precipitations can be ascribed to the high frequency loading effect. In general, the lattice fringe-like precipitation has a higher elastic modulus compared to the glass matrix. It is well established that when polymers with disorder structure are blended together, the dynamic modulus E' of the composite are often found to obey the "rule of mixtures" [31]:

$$E_c(T) = \sum_i \varphi_i E_i(T) \tag{1}$$

where φ_i denotes the volume fraction of the ith component and E_i its modulus at temperature T. Similarly, for MG, the modulus measured by DMA can be regarded as a mixture modulus of the ordered and amorphous phases. The widely distributed lattice fringe-like precipitations contribute to the increase of the storage modulus at a proper condition.

In addition, the apparent storage modulus that can be efficiently modified is associated with the lattice fringe-like precipitations and the high-temperature induced disordered cohesive element (liquid-like zone). The fully disordered sample that became partly ordered after the LSP treatment at RT shows a higher storage modulus upon subsequent dynamic thermal-mechanical loading. A similar result can be obtained in cyclic loading with 0.4% elastic strain of the ZrCuFeAl MG [27]. Both cases show that the mechanical loading can result in the generation of a crystal-like ordered structure, which disappears upon subsequent heating near the T_g. The structural transitions modify the behaviors of the storage modulus without affecting the rheological behavior. However, the change of the storage modulus may be insensitive at a lower frequency due to the different time scales for structural relaxation.

In fact, the appearance of the pre-existing local precursor could significantly affect the dynamic viscoelastic behavior of MGs. The variations of $\ln(\tan\delta)$ vs the frequency and temperature at various temperatures before and after the LSP treatment are shown in Fig. 3. According to the quasi-point defect (QPD) model, the $\ln(\tan\delta)$ can be expressed as [32–34]:

$$\ln(\tan\delta) = -\frac{E_a}{KT} - \chi\ln\omega - \chi\ln\tau^* + \lambda \tag{2}$$
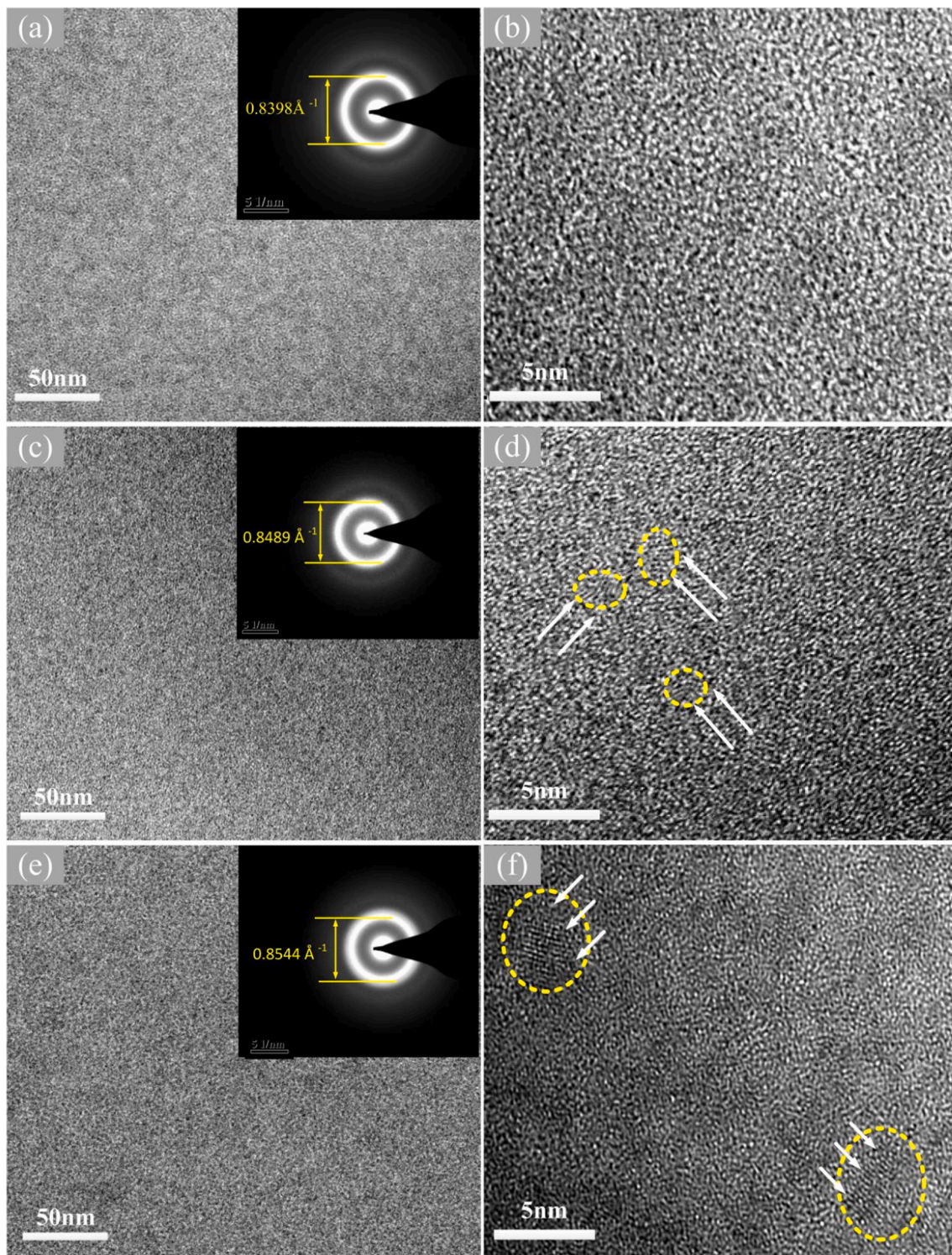
Fig. 2. . Changes in bright field images: (a) as-cast, (c) LSP-treated, (e) as-cast continuously heated up to 633 K at a frequency of 16 Hz in the DMA test. Inserts: corresponding selected area electron diffraction pattern. HRTEM images: (b) as-cast, (d) LSP-treated, (f) as-cast continuously heated up to 633 K at a frequency of 16 Hz in the DMA test. The local ordered structure in nanometers scale is seen in the HRTEM images.

where E_a denotes the apparent activation energy, and K is the Boltzmann constant, λ is a constant, ω is the angular frequency, χ is a correlation factor ranging from 0 (full order) to 1 (full disorder), which is linked to the quasi-point defect concentration. $\tau^* = t_0(\tau_\beta/t_0)^{1/\chi}$, t_0 is a time scale parameter, τ_β is the mean activation time of one structural unit, Within the framework of this model, the system remains in an iso-structural state when the temperature is below T_g, meaning that the correlated

factor χ is constant [32]. As shown in Fig. 3 (a), the slope χ in the low-frequency region retains a constant value which is consistent with the predictions of the QPD theory. With the increased frequency, it transforms into a non-linear dependency, which does not fully obey the above-mentioned model. This phenomenon becomes more severe for samples after the LSP treatment. As shown in Fig. 3 (b), the nonlinear transformation occurs prematurely towards the lower frequency region.
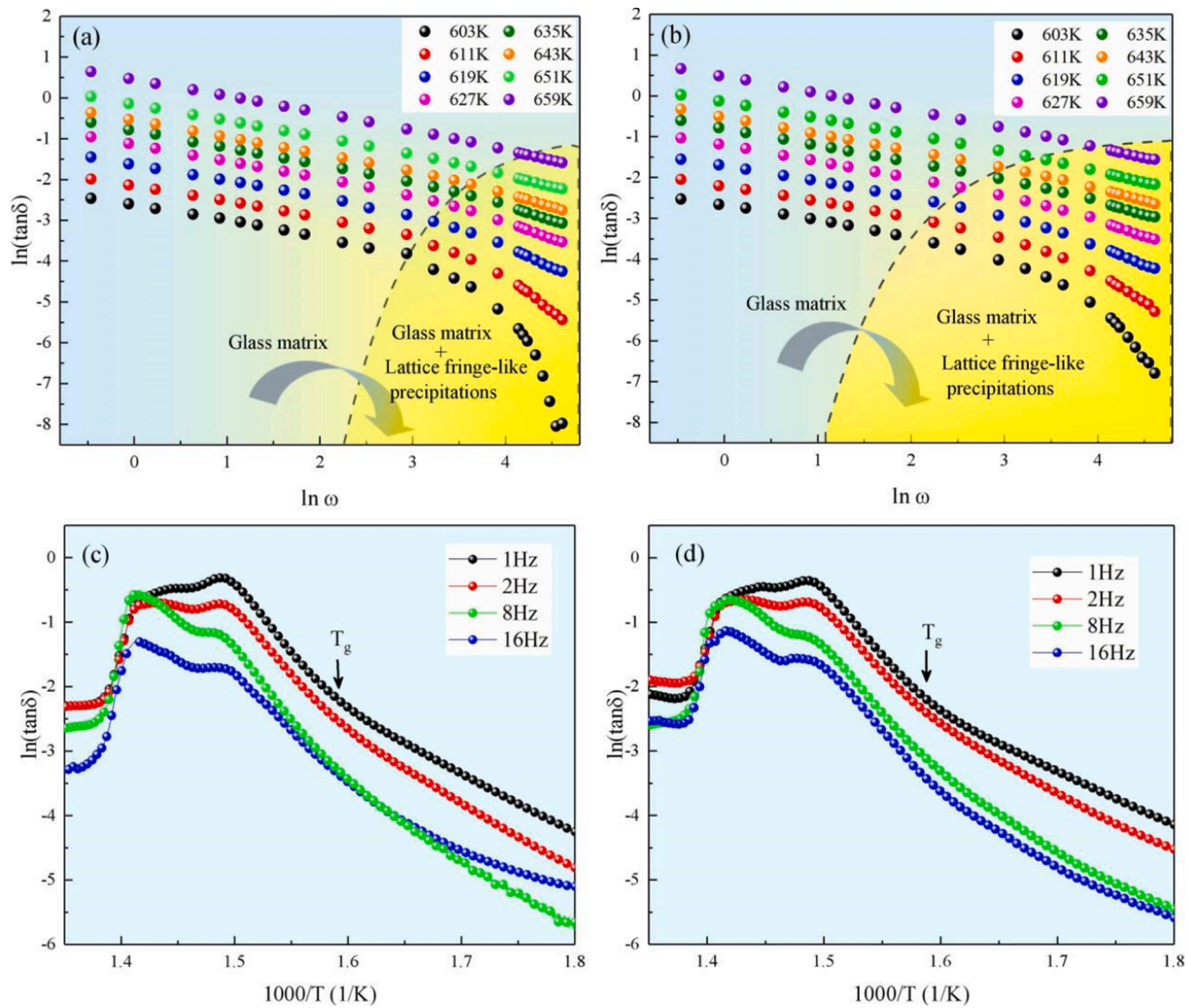
Fig. 3. . Frequency dependence of the loss factor tan δ of (a) as-cast and (b) LSP-treated samples. The relationship between the internal friction $\ln(\tan\delta)$ and 1000/T for (c) as-cast samples and (d) LSP-treated samples.

However, the microstructural evolution of MGs during dynamic mechanical loading is a thermal-mechanical coupling process, which is induced by both the external thermally-activated effect and mechanical cycling excitation. A larger loading frequency can significantly influence the apparent activation energy of diffusion and nucleation, which can subsequently lead to partial nanocrystallization of MGs. The higher the loading frequency is, the more likely the crystallization is to occur [27]. On the other hand, when the MG is subjected to the LSP treatment, the stress wave is decomposed into two states, namely the shear stress along the maximum shear plane and the hydrostatic compression in the impact direction [35]. The shear stress causes the atoms to move along the shearing direction, thereby leading to an increase in the free volume associated with atomic dilatation [36]. However, the hydrostatic compressive stress can decrease the energy barrier of MGs for crystallization, which in turn results in increased nucleation rate and leads to the occurrence of the ordered phase [37]. The values of $\ln(\tan\delta)$ vs. 1000/T for samples before and after LSP are displayed in Fig. 3 (c) and (d). When temperature is below T_g, it is noted that the internal friction of as-cast MGs with low-frequency loading (1, 2, 8 Hz) increases linearly with increased temperature, exhibiting an obvious elastic relaxation behavior. Instead, high-frequency loading (16 Hz) can induce power-exponential function distribution of $\ln(\tan\delta)$, which results from the appearance of the lattice fringe-like precipitations. It should be noted that the dynamical response of the pre-existing local precursor is also observed in the LSP-treated sample, as shown in Fig. 3 (b).

Due to the limitations of the experimental conditions, the dynamic response within the frequency range across several orders of magnitude is difficult to obtain. Therefore, a master curve within a wide frequency range is obtained based on the time-temperature equivalence principle [38]. Firstly, a set of frequency spectra under different temperature were measured in the same frequency range. Then, the frequency spectra at a given temperature was took as a reference line, the others move horizontally to obtain the master curve. For simplicity, 633 K was selected as the reference temperature of the axial, A typical master curve of the storage modulus E'/Emax in MG before and after the LSP treatment is shown in Fig. 4(a). It reveals that the LSP-treated sample has a lower storage modulus in the low-frequency region, but exhibits a higher storage modulus in the high-frequency region, which is consistent with the results in Fig. 1. For loss modulus, after LSP, the peak of loss modulus shifts to a lower frequency region obviously, as shown in Fig. 4 (b). Since the relaxation time is close to the reciprocal of the frequency, the lower frequency implys lower atomic mobility and longer characteristic relaxation time at the same temperature, which is inconsistent with previous reports [39,40]. Based on the QPD theory, the structure of the amorphous material is frozen when the temperature is below T_g [32], which considers that the local movements can only occur in the "weak spot" when the material obtains activation energy from outside, thus the systems should be softening with higher atomic mobility. Certainly, the TEM results provide an appropriate alternative explanation. The MGs can be viewed as tightly bonded atomic clusters that overlap to form the
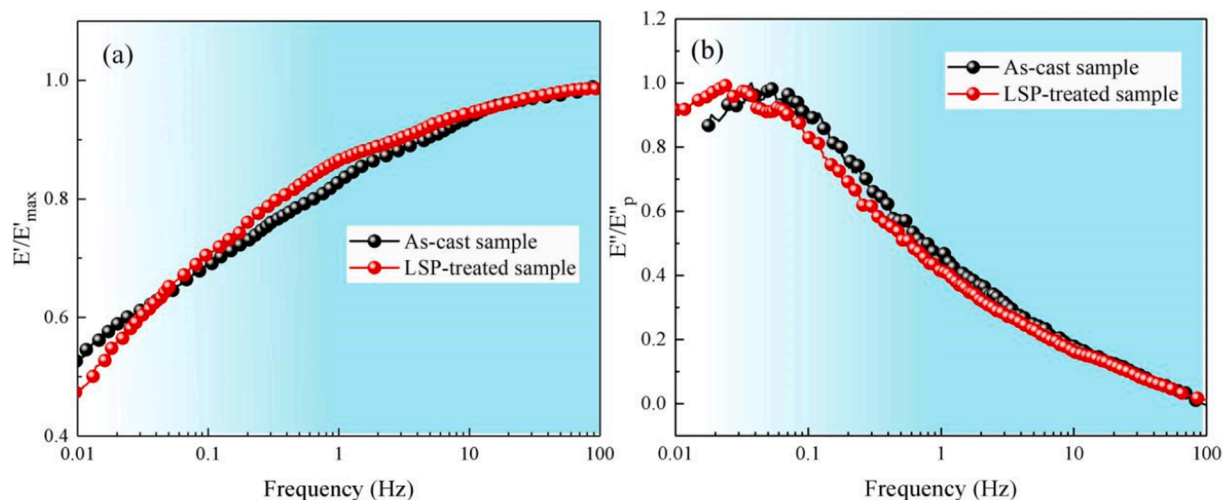
Fig. 4. . Master curves of the Zr-based MG before and after LSP treatment for (a) storage modulus E'/E_{max} and (b) loss modulus E''/E_p, where E_{max} is the maximum value of the storage modulus in the master curve, E_p is the peak value of the loss modulus in the master curve.

percolating "skeleton" of the glassy structure with loosely bonded liquid-like regions when subjected to the pre-deformed treatment [41], which is also referred to as "mechanical rejuvenation". The LSP treatment can bring in a large number of liquid-like regions in the glass matrix due to the shear stress. Furthermore, the high pressure of the laser shock wave can significantly reduce the activation energy barrier for crystal nucleation, which is confirmed by the appearance of the lattice fringe-like precipitations of MGs after the LSP treatment. The abnormal increase in the storage modulus of MGs after LSP could result as a consequence of the competition between the liquid-like region change and the pre-existing fringe-like precipitations.

4. Conclusion

The dynamic mechanical properties of Zr-based MG before and after LSP treatment were investigated. An abnormal increase in the storage modulus near the T_g after LSP was observed, which was related to the appearance of the lattice fringe-like precipitations with several nanometers. The fully disordered sample, which became partly ordered after the LSP treatment at RT, shows a higher storage modulus upon subsequent dynamical thermal-mechanical loading. An increased deviation between the dynamic mechanical result and QPD theory prediction was observed at high frequency or after LSP treatment due to the effect of pre-existing local precursors. The equivalency of the time and temperature method was induced to explain the abnormal increase of the storage modulus based on the pre-existing local fringe-like precipitations and the liquid-like region change from the perspective of the atomic movement. The results provide insightful information on the microstructural changes and viscoelastic properties of the MGs after LSP treatment.

5. Data availability

The datasets generated during and/or analyzed during the current study are available from the corresponding author on reasonable request.

Declaration of Competing Interest

The authors declare that they have no known competing financial interests or personal relationships that could have appeared to influence the work reported in this paper.

Appendix A. Supplementary data

Supplementary data to this article can be found online at https://doi.org/10.1016/j.optlastec.2020.106875.

References

[1] Y. Liao, C. Ye, G.J. Cheng, A review: warm laser shock peening and related laser processing technique, Opt. Laser. Technol. 78 (2016) 1–24.

[2] M. Achintha, D. Nowell, D. Fufari, E.E. Sackett, M.R. Bache, Fatigue behaviour of geometric features subjected to laser shock peening: experiments and modelling, Int. J. Fatigue 62 (2014) 171–179.

[3] A. Gujba, M. Medraj, Laser peening process and its impact on materials properties in comparison with shot peening and ultrasonic impact peening, Materials 7 (2014) 7925–7974.

[4] E. Williams, N. Lavery, Laser processing of bulk metallic glass: a review, J. Mater. Process. Technol. 247 (2017) 73–91.

[5] L. Petan, J.L. Ocaña, J. Grum, Influence of laser shock peening pulse density and spot size on the surface integrity of X2NiCoMo18-9-5 maraging steel, Surf. Coat. Tech. 307 (2016) 262–270.

[6] X.C. Zhang, Y.K. Zhang, J.Z. Lu, F.Z. Xuan, Z.D. Wang, S.T. Tu, Improvement of fatigue life of Ti-6Al-4V alloy by laser shock peening, Mater. Sci. Eng. A 527 (2010) 3411–3415.

[7] C. Wang, L. Wang, C.L. Wang, K. Li, X.G. Wang, Dislocation density-based study of grain refinement induced by laser shock peening, Opt. Laser Technol. 121 (2020) 105827.

[8] S. Prabhakarana, A. Kulkarni, G. Vasanthb, S. Kalainathan, P. Shuklac, V. K. Vasudevan, Laser shock peening without coating induced residual stress distribution, wettability characteristics and enhanced pitting corrosion resistance of austenitic stainless steel, Appl. Surf. Sci. 428 (2018) 17–30.

[9] S. Kalainathan, S. Prabhakaran, Recent development and future perspectives of low energy laser shock peening, Opt. laser Technol. 81 (2016) 137–144.

[10] P. Peyre, R. Fabbro, Laser shock processing: a review of the physics and applications, Opt. Quant. Electron. 27 (1995) 1213–1229.

[11] S.J. Lainé, K.M. Knowles, P.J. Doorbar, R.D. Cutts, D. Rugg, Microstructural characterisation of metallic shot peened and laser shock peened Ti-6Al-4V, Acta Mater. 123 (2017) 350–361.

[12] Y.S. Li, Y.P. Wei, Y, K. Zhang, Y. Wang, W.Q. Tang, B.C. Wei, Rejuvenation, embryonic shear bands and improved tensile plasticity of metallic glasses by nanosecond laser shock wave, J. Non-Cryst. Solids 513 (2019) 76-83.

[13] Y.F. Cao, X. Xie, J. Antonaglia, B. Winiarski, G. Wang, Y.C. Shin, P.J. Withers, K. A. Dahmen, P.K. Liaw, Laser shock peening on Zr-based bulk metallic glass and its effect on plasticity: experiment and modeling, Sci. Rep. 5 (2015) 10789.

[14] J. Fu, Y.H. Zhu, C. Zheng, R. Liu, Z. Ji, Evaluate the effect of laser shock peening on plasticity of Zr-based bulk metallic glass, Opt. laser Technol. 73 (2015) 94–100.

[15] L. Wang, Y.K. Zhao, L. Wang, Z.H. Nie, B.P. Wang, Y.F. Xue, H.F. Zhang, H. Fu, D. E. Brown, Y. Ren, In-situ synchrotron X-ray diffraction study of dual-step strain variation in laser shock peened metallic glasses, Scripta Mater. 149 (2018) 112–116.

[16] Y. Zhu, J. Fu, C. Zheng, Z. Ji, Structural and mechanical modifications induced on Zr-based bulk metallic glass by laser shock peening, Opt. Laser Technol. 86 (2016) 54–60.

[17] Y.S. Li, K. Zhang, Y. Wang, W.Q. Tang, Y.T. Zhang, B.C. Wei, Z. Hu, Abnormal softening of Ti-metallic glasses during nanosecond laser shock peening, Mater. Sci. Eng. A 773 (2020) 138844.

[18] A. Slipenyuk, J. Eckert, Correlation between enthalpy change and free volume reduction during structural relaxation of $Zr_{55}Cu_{30}Al_{10}Ni_5$ metallic glass, Scripta Mater. 50 (2004) 39–44.

[19] Y.P. Wei, G.Y. Xu, K. Zhang, Z. Yang, Y.C. Guo, C.G. Huang, B.C. Wei, Anomalous shear band characteristics and extra-deep shock-affected zone in Zr-based bulk metallic glass treated with nanosecond laser peening, Sci. Rep. 7 (2017) 43948.

[20] Y.S. Li, K. Zhang, G.H. Duan, G.Y. Xu, Y.H. Wei, Y.P. Wei, B.C. Wei, Effect of laser shock peening on the surface morphology of metallic glasses, Mater. Sci. Forum 898 (2017) 689–695.

[21] G.Y. Xu, Y.P. Wei, B.C. Wei, Deformation feature and properties of Zr based bulk metallic glass treated by laser shock peening, Mater. Res. Innovations 798 (2014) 798–802.

[22] A.P. Srivastava, T. Stefanov, D. Srivastava, D.J. Browne, Multiple relaxation processes in $Zr_{44}Cu_{40}Al_8Ag_8$ bulk metallic glass, Mater. Sci. Eng. A 651 (2016) 69–74.

[23] J.C. Qiao, J.M. Pelletier, H.C. Kou, X. Zhou, Modification of atomic mobility in a Ti-based bulk metallic glass by plastic deformation or thermal annealing, Intermetallics 28 (2012) 128–137.

[24] J.M. Pelletier, Dynamic mechanical properties in a $Zr_{46.8}Ti_{13.8}Cu_{12.5}Ni_{10}Be_{27.5}$ bulk metallic glass, J. Alloy Compd. 393 (2005) 223–230.

[25] K.S.N. Satish Idury, P. Rastogi, R.L. Narayan, N. Singh, K.R. Ravi, B.S. Murty, J. Bhatt, Room temperature dynamic indentation response of partially crystallized Zr-Cu Metallic Glass, J. Alloy Compd. 834 (2020) 155161.

[26] G.J. Lyu, J.C. Qiao, J.M. Pelletier, L. Zhang, H.F. Zhang, Y. Yao, Dynamic mechanical behaviors of a metastable b-type bulk metallic glass composite, J. Alloy Compd. 819 (2020) 153040.

[27] D.V. Louzguine-Luzgin, M.Yu. Zadorozhnyy, S.V. Ketov, J. Jiang, I.S. Golovin, A. S. Aronin, Influence of cyclic loading on the structure and double-stage structure

[28] J. Kong, Z. Ye, W. Chen, X. Shao, K. Wang, Q. Zhou, Dynamic mechanical behavior of a Zr-based bulk metallic glass composite, Mater. Design 88 (2015) 69–74.

[29] H. Chen, Y. Hai, R. Liu, Q. Lei, L. Ye, J. Xu, G. Wang, W. Yin, L. Yan, X.T. Zhou, The microstructure and mechanical properties of He^+ ion irradiated $Zr_{55}Cu_{30}Al_{10}Ni_5$ bulk metallic glass, Intermetallics 104 (2019) 52–58.

[30] S. Cheng, C. Wang, M. Ma, D. Shan, B. Guo, Mechanism for microstructural evolution induced by high temperature deformation in Zr-based bulk metallic glasses, J. Alloy Compd. 676 (2016) 299–304.

[31] K.D. Ziegel, A. Romanov, Modulus reinforcement in elastomer composites. II. Polymeric fillers, J. Appl. Polym. Sci. 17 (1973) 1133-1142.

[32] J. Perez, Quasi-punctual defects in vitreous solids and liquid-glass transition, Solid State Ionics 39 (1990) 69–79.

[33] J.C. Qiao, J.M. Pelletier, Mechanical relaxation in a Zr-based bulk metallic glass: analysis based on physical models, J. Appl. Phys. 112 (2012) 033518.

[34] Z.F. Yao, J.C. Qiao, J.M. Pelletier, Y. Yao, Characterization and modeling of dynamic relaxation of a Zr-based bulk metallic glass, J. Alloy Compd. 690 (2017) 212–220.

[35] S.W. Lee, M.Y. Huh, E. Fleury, J.C. Lee, Crystallization-induced plasticity of Cu–Zr containing bulk amorphous alloys, Acta Mater. 54 (2006) 349–355.

[36] F. Spaepen, A microscopic mechanism for steady state inhomogeneous flow in metallic glasses, Acta Metall. 25 (1977) 407–415.

[37] F. Ye, K. Lu, Pressure effect on crystallization kinetics of an Al-La-Ni amorphous alloy, Acta Mater. 47 (1999) 2449–2454.

[38] W. Zhai, C.H. Wang, J.C. Qiao, J.M. Pelletier, F.P. Dai, B. Weil, Distinctive slow β relaxation and structural heterogeneity in (LaCe)-based metallic glass, J. Alloy Compd. 742 (2018) 536–541.

[39] J.C. Qiao, J.M. Pelletier, C. Esnouf, Y. Liu, H. Kato, Impact of the structural state on the mechanical properties in a Zr–Co–Al bulk metallic glass, J. Alloy Compd. 607 (2014) 139–149.

[40] J.C. Qiao, R. Casalini c,J.M. Pelletier, Main (α) relaxation and excess wing in Zr50Cu40Al10 bulk metallic glass investigated by mechanical spectroscopy, J. Non-Cryst Solids 407 (2015) 106-109.

[41] J.C. Ye, J. Lu, C.T. Liu, Q. Wang, Y. Yang, Atomistic free-volume zones and inelastic deformation of metallic glasses, Nat. Mater. 9 (2010) 619–623.